

Title

Damage behavior of CFRP subjected to simulated lightning current under air, reduced-pressure air, and N₂ environments

Authors

Shintaro Kamiyama¹, Yoshiyasu Hirano², Takao Okada², Koji Sawaki³, Takeo Sonehara⁴, Toshio Ogasawara^{1*} (* corresponding author)

1. Tokyo University of Agriculture and Technology
2. Japan Aerospace Exploration Agency (JAXA)
3. Nagoya University
4. Shoden Corporation

Corresponding author *:

Toshio Ogasawara
Professor, Department of Mechanical Systems Engineering
Tokyo University of Agriculture and Technology
2-24-16, Naka-cho, Koganei-shi, Tokyo, Japan
ogasat@cc.tuat.ac.jp

Abstract

This study examined lightning strike damage behaviors of carbon fiber reinforced plastic (CFRP) laminates under air (0.1 MPa), reduced-pressure air (0.02 MPa), and N₂ (0.1 MPa) environments to elucidate the effects of atmospheric environments on lightning damage. Simulated lightning current in accordance with SAE-ARP 5412B was applied to each specimen. The maximum current peak value was defined as 40 kA. CFRP laminates under reduced-pressure air (0.02 MPa) exhibited slight damage compared with that under atmospheric-pressure air. By contrast, CFRP laminates under N₂ sustained considerably more damage than under air (0.1 MPa). High-speed observations revealed that the atmospheric gas and pressure affect the arc root behavior. Finite element analysis was conducted based on experimentally obtained results to model lightning strike damage. The arc root length captured using a high-speed camera was incorporated into the analytical model. Numerical analysis results showed good correspondence with experimentally obtained results. These experimental and analytical results indicate that arc root behavior strongly affects lightning strike damage.

Keywords

Lightning strike damage, Electrical properties, Thermal properties, Delamination, Finite element analysis (FEA),

1. Introduction

Carbon fiber reinforced plastic (CFRP) has been applied widely to primary aircraft structures because of its high specific strength and stiffness. It is widely understood that CFRP is severely damaged by lightning compared to metallic materials. Therefore, lightning strikes

during operation pose a severe hazard to aircraft. For that reason, CFRP structures require special design to reduce the threat of lightning strike damage. Metal mesh such as expanded copper foil (ECF) is often applied to the surfaces of CFRP structures as a lightning strike protection (LSP) system [1, 2]. In fact, LSP is effective to suppress lightning strikes, but complete protection remains elusive. Once a composite aircraft structure is damaged by a lightning strike, inspection and/or repair must be done, thereby affecting the aircraft operation. Understanding details of lightning strike damage mechanisms is therefore important for developing aircraft structures using CFRP and for further improvement of safety.

The damage behavior of CFRP laminates struck by lightning has been assessed experimentally in some earlier works [3–8]. These works reported diverse manifestations of lightning-associated degradation such as delamination, matrix cracking, carbon fiber breakage, and thermal decomposition of matrix resin. Moreover, numerical analyses have been conducted by solving electrical and thermal equations [9–16]. Areas showing raised temperatures by numerical analysis roughly agree with actual damaged areas. Lightning strike events occur in an extremely short time. Moreover, lightning strike damage can be caused by complex electrical, thermal, and mechanical phenomena such as Joule heating, thermal decomposition of matrix resin, combustion, shock waves, and Lorentz force [17]. These phenomena are complicated. Therefore, details of the effects of each phenomenon and interaction of these phenomena on lightning strike damage have not been clarified. Especially, the effects of atmospheric gas and pressure on the CFRP damage when exposed to impulse current have not been evaluated in the relevant literature. The testing environment affects the combustion of carbon fiber, matrix resin, and pyrolysis gas, progression of the arc attachment area, behaviors of surface discharge and acoustic force, and others. Understanding the effects of these phenomena on lightning strike damage is extremely important to elucidate damage mechanisms and testing methods.

The objective in this study is investigation of the effects of atmospheric environment on lightning damage behavior of CFRP laminates of three kinds. To achieve this objective, simulated lightning current tests were conducted under environments of three kinds: atmospheric-pressure air (0.1 MPa), reduced-pressure air (0.02 MPa), and atmospheric pressure nitrogen (N₂, 0.1 MPa). We evaluated CFRP with the same carbon fiber and resins of three kinds (CF/epoxy, CF/ bismaleimide (BMI) and CF/ polyetheretherketone (PEEK)), which were reported from our earlier work [18]. Lightning strike damage behavior was observed during the simulated lightning testing using a video camera and a high-speed camera. After the testing, lightning strike damage on the surface was visually assessed. Subsequently, the internal damage was evaluated by ultrasonic inspection. Coupled thermal–electrical analysis and heat transfer analysis based on finite element analysis were conducted for the CF/epoxy. Damage mechanisms caused by lightning strikes in atmospheric-pressure air and reduced-pressure air were discussed.

2. Experimental

2.1 Materials and specimens

Cross-ply laminates of CF/epoxy (IMS60/#133), CF/BMI (IMS60/#304), and CF/PEEK (IMS60/Victrex PEEK 150G), to which same PAN-type carbon fiber (IMS60) were applied, were used for the simulated lightning strike tests. Unidirectional prepreg tapes obtained from Teijin Co. Ltd., Japan were laminated to [0/90]_{4s}, and were molded using an autoclave or

a hot press. Each specimen had 150 mm width and 150 mm length. The thicknesses of CF/epoxy, CF/BMI and CF/PEEK were, respectively, 2.2 mm, 2.1 mm, and 2.2 mm. The fiber volume fraction calculated using the fiber areal weight and specimen thickness were, respectively, 59%, 62%, and 59%. The CF/epoxy, CF/BMI, and CF/PEEK properties are presented in Table 1.

2.2 Simulated lightning current tests under different atmospheres

An impulse current generator (Otowa Electric Co., Ltd., Japan) at the National Composite Center, Nagoya University, Japan was used for simulated lightning current testing (Fig. 1(a)). Impulse current tests were conducted under air (0.1 MPa), reduced-pressure air (0.02 MPa) and N₂ (0.1 MPa) to clarify the effects of atmospheric environment on lightning strike damage. The tests were conducted in an acrylic chamber of 380 mm diameter and 390 mm height, as shown in Fig. 1(b). A schematic drawing of the test equipment around the chamber is shown in Fig. 2. Under atmospheric-pressure air (0.1 MPa), the lid at the chamber top was fixed with bolts after fixing the specimen to the jig. Under reduced pressure of air, experiments were conducted using a rotary vane vacuum pump to set the pressure inside the chamber to 20% atmospheric pressure (0.02 MPa). In the N₂ environment, the chamber interior was evacuated using a rotary vane vacuum pump; then N₂ gas with purity of 99.99% was charged into the chamber. The test was conducted under atmospheric pressure (0.1 MPa) while flowing N₂ gas into the chamber at a flow rate of 1.2 L/min.

The outer edge of specimen was fixed in a copper jig which was electrically connected to ground. A positive impulse current was applied to the central part of the specimen from a needle-type discharge probe. The distance separating the discharge probe tip from the specimen was 2 mm.

Lightning strike damage behavior was observed using a video camera (HDR-CX520; Sony Corp.) at 30 fps, and using a high-speed camera (HPV-1; Shimadzu Corp.) at 250 kfps. Ultrasonic inspection was conducted from the back surface using an ultrasonic device (HIS-3; Krautkramer Japan Co. Ltd., Japan) to evaluate internal damage (delamination). The scanning pitch was 0.50 mm × 0.50 mm. The scanning probe operated at 3.5 MHz frequency.

2.3 Simulated lightning current waveform

The lightning waveform defined in SAE-ARP 5412B is used to evaluate the lightning resistivity of aircraft structures [19]. The component A waveform, which simulated the initial stroke, was applied to specimens (Fig. 3). The component A waveform is expressed with the current peak value (I_{peak}), the front time from the nominal origin to I_{peak} (T_1), and the duration from the nominal origin to 50% I_{peak} through I_{peak} (T_2) as parameters. In addition, the action integral, defined as $\int_0^t i^2 dt$ was used to evaluate the lightning waveform quantitatively. Therein, i and t respectively signify the electrical current and time. The action integral denotes a value that is proportional to the electrical energy. The current peak value is defined as 200 kA in SAE-ARP 5412B. However, that was modified to 40 kA for this study because of specimen size. T_1/T_2 was approximately 28/86 μ s. The lightning waveform conditions for the respective specimens are presented in Table 2.

3. Experimental results and discussion

3.1 Lightning strike damage observation using a video camera and a high-speed camera

Fig. 4 shows typical images, captured using a video camera, of CF/epoxy at 0.1, 0.5, and 1.0 s after application of impulse current. In air (0.1 MPa), flame was observed at the time of impulse current application. The flame disappeared at 3 s after the impulse current application. White smoke was observed for several seconds. No flame was observed under reduced-pressure air (0.02 MPa) or N₂. However, white smoke was observed for several seconds immediately after application of impulse current under N₂.

Fig. 5 shows high-speed images, captured using a high-speed camera, of CF/epoxy at 20, 52, and 100 μs after impulse current application. The impulse current was applied to each specimen during approximately 136 μs, as shown in Fig. 3(b). Pyrolysis gas was observed at the time when the impulse current was applied. In air (0.1 MPa) and N₂, pyrolysis gas was generated along the transverse direction (90°) of the top layer from the arc attachment point. However, under reduced-pressure air (0.02 MPa), the pyrolysis gas progressed in the transverse direction (90°) of the top layer. It connected to the copper jig at 24 μs. This phenomenon was observed in CF/BMI and CF/PEEK under reduced-pressure air (0.1 MPa).

3.2 Evaluation of lightning strike damage

Fig. 6 shows the arc attachment surface of test specimens after the impulse current tests. Carbon fibers in the CF/epoxy were broken around the arc attachment area. An internal layer was exposed because of the lifting-up of the top surface along the longitudinal direction (0°). The lengths of carbon fiber breakage in the transverse direction of the top layer were approximately 135 mm and 120 mm, respectively, under air (0.1 MPa) and N₂. Carbon fiber breakage was not observed on the surface under reduced-pressure air (0.02 MPa). Carbon fiber breakage in the CF/BMI was observed radially around the arc attachment point. In air (0.1 MPa) and N₂, delamination was observed on the top layer along the longitudinal direction, but no delamination was observed under reduced-pressure air (0.02 MPa). Moreover, thermal decomposition of the matrix resin was observed. In the CF/PEEK, carbon fibers were exposed because of thermal decomposition of the matrix resin around arc attachment point under air (0.1 MPa) and N₂. No damage such as carbon fiber breakage or thermal decomposition of matrix resin was observed on the back surface of the specimens (CF/epoxy, CF/BMI, and CF/PEEK) under any test conditions.

The ultrasonic inspection results are portrayed in Fig. 7. Right and left sides were reversed in Fig. 7 for direct comparison with Fig. 6. The internal damage area inferred from ultrasonic C-scanning results is presented in Table 3. In the CF/epoxy, delamination was detected within approximately 0.7 mm (5 layers) from the front surface under atmospheric-pressure air (0.1 MPa). Under reduced-pressure air (0.02 MPa), no significant delamination was observed. Under N₂ (0.1 MPa), delamination was detected within approximately 1.1 mm (8 plies), which was deeper than that under atmospheric-pressure air. In the CF/BMI, delamination was detected within approximately 0.2 mm (2 plies) and approximately 0.8 mm (6 plies) under atmospheric-pressure air (0.1 MPa) and N₂. Nevertheless, no significant delamination was observed under reduced-pressure air. In the CF/PEEK, no significant delamination was observed under any atmospheric condition.

3.3 Discussion

First, lightning strike behavior under atmospheric-pressure air (0.1 MPa) and reduced-pressure air (0.02 MPa) are discussed. Experimental results demonstrate that lightning strike damage under reduced-pressure air (0.02 MPa) was much less than that under air (0.1 MPa). High-speed observation results indicate that the impulse current was discharged directly from the probe to the copper jig at the edge of a specimen after 24 μ s. That result implies that little electric current flows inside the CFRP. By this phenomenon, electric current progresses as surface discharge on the material surface [20]. In addition, under reduced-pressure air, the influence of the mechanical load by the plasma gas (shock wave) is presumed to be much less than those under atmospheric-pressure air. This might be one reason that less damage occurred than under atmospheric air.

Next, the N₂ effects on lightning strike damage are discussed. The damage of CF/epoxy and CF/BMI under N₂ was greater than that under air (0.1 MPa). Moreover, in the CF/PEEK, no significant difference was found in internal damage caused by lightning strike under air (0.1 MPa) and N₂. However, the thermal decomposition area on the arc attachment surface was larger under N₂ than in air (0.1 MPa). That result implies that the effects of heat generation from the combustion of pyrolysis gas are not meaningful because the damage under N₂ was not suppressed compared with that under air (0.1 MPa). The high-speed observation results and the damage after application of impulse current suggest that the arc root area propagated along the transverse direction (90°) of the top layer in the CF/epoxy.

Fig. 8 shows high-speed images of the arc root length along the transverse direction (90°) of the top layer in the CF/epoxy in each atmospheric environment. The results imply that the arc root progressed longer and increased for a longer time under air than under N₂. Therefore, the impulse current flows locally near the arc attachment point under N₂. Consequently, the increased current density around the arc attachment point led to increased damage.

Further studies must be conducted to clarify the mechanisms of arc root change under different test environments. However, these experimentally obtained results suggest that arc root changes on the arc attachment surface affect lightning strike damage.

4. Lightning strike damage simulation of CF/epoxy

As explained in this section, coupled thermal–electrical analysis and heat transfer analysis considering pyrolysis reaction of CFRP were conducted to elucidate arc root behavior and its effects on the lightning strike damage. The basic methodology was reported in the literature by our research group [9, 16]. Lightning strike damage of CF/epoxy under atmospheric-pressure air (0.1 MPa) and reduced-pressure air (0.02 MPa) was incorporated into the numerical calculation model.

4.1 FEA model and boundary conditions

A commercial FEA solver (ABAQUS/Standard 2017, Simulia; Dassault Systemes, France) was used for numerical simulation. During application of the impulse current (0–136 μ s), coupled thermal–electrical analysis was conducted. As the first step of coupled thermal–electrical analysis, the electrical potential inside the specimen was calculated under appropriate boundary conditions, as described later. Joule heat generation was calculated for each element. For the next step, the temperature distribution was obtained by conducting transient heat transfer analysis under appropriate thermal boundary conditions. The degree of pyrolysis was calculated for each element using the obtained temperature distribution. An ABAQUS user subroutine,

USDFLD, was used to calculate the degree of pyrolysis. At the same time, the electrical conductivity in each element was updated in each increment corresponding to the degree of pyrolysis. By repeating the analytical procedure for each increment, the coupled thermal–electrical analysis considering the pyrolysis behavior of CFRP was achieved.

During cooling (30 s), transient heat transfer analysis was conducted to assess the effects of heat soak-back after the impulse current application. The initial temperature distribution of heat transfer analysis was defined as that obtained from coupled thermal–electrical analysis at the final increment. Then, the degree of pyrolysis was calculated similarly to that for the coupled thermal–electrical analysis.

The FEA model is shown in Fig. 9. A quarter of cross-ply laminates were modeled to consider symmetry. Materials in FEA were identical to those used for simulated lightning current testing. Material properties reported from an earlier study [9, 16] were used for FEA. The impulse current profile with a maximum current of 40 kA, which was obtained from the experiments, was applied to the center of the specimen as an electrical boundary condition of coupled thermal–electrical analysis. To consider time-dependent arc root behavior, the arc root area was defined as follows, from reference to an earlier study [21]. The impulse current applied area was assumed to be elliptical. The arc root length was assumed to change linearly with time (Fig. 10). The electrical load area was changed stepwise every 8 μs . In all, 17 surface current loads were applied. The major axis (2b) of the ellipse was assumed to be 10 times longer than the minor axis (2a) in Fig. 9 because of observation results of the arc attachment surface. Under reduced-pressure air (0.02 MPa), high-speed camera observations indicate that the impulse current was applied to the top surface of the CFRP specimen for up to 24 μs . However it was discharged directly to the copper jig at the edge of the specimen from the discharge probe after 24 μs . Therefore, electrical current was applied within 24 μs for the simulation under reduced-pressure air (0.02 MPa). Other boundary conditions were the same as those reported from earlier studies [9, 16].

4.2 Numerical analysis results and discussion

Figs. 11(a) show superimposed images showing damage for each layer at 30 s (the thermal decomposition was estimated as be finished). Contour plots show the distance from the back surface to compare ultrasonic inspection results. The numerical analysis results are mirrored for direct comparison with the experimentally obtained results because a quarter model was used for FEA in this study. A degree of pyrolysis of 100% indicates that the matrix resin of CFRP was thermally decomposed completely. The area in which the pyrolysis degree exceeded 0% was assumed as the damage area (delamination) caused by the lightning strike.

First, the damage in the through-thickness direction is discussed. The thermally decomposed area was approximately five layers from the surface under air (0.1 MPa), although it occurred only at the arc attachment surface under reduced-pressure air (0.02 MPa). The damaged area in through-thickness direction estimated by FEA almost agreed with the experimentally obtained results. The net action integrals applied to CFRP were approximately 90 kA^2s and 10 kA^2s , respectively, under air and reduced-pressure air. Therefore, the small action integral reduces the pyrolysis area created by lightning strike.

Next, the lightning strike damage shape can be discussed. Numerical analysis results obtained under air (0.1 MPa) roughly agree with experimentally obtained results. However, the

damage on the arc attachment surface was greater and the internal damage was less than that indicated by experimentally obtained results. These results indicate that delamination during application of impulse current affects the lightning strike damage behavior. Numerical analysis results obtained under reduced-pressure air (0.02 MPa) indicate that no damage occurs around the arc attachment point. This result indicates that the time-dependent current density was not modeled appropriately. Moreover, this result suggests that mechanical loading caused by a shock wave, Lorentz force, or thermal flux from the arc can also affect lightning strike damage, although this study assessed none of those factors.

5. Conclusions

This study examined atmospheric environment effects on lightning strike damage behavior. Lightning strike damage behavior of CF/epoxy, CF/BMI, and CF/PEEK was investigated under air (0.1 MPa), reduced-pressure air (0.02 MPa), and N₂ (0.1 MPa). The following results were obtained.

- (1) Lightning strike damage such as carbon fiber breakage, color change, and delamination under reduced-pressure air (0.02 MPa) was slight compared to that occurring under atmospheric-pressure air (0.1 MPa).
- (2) The lightning strike damage under N₂ (0.1 MPa) was slightly greater than that under atmospheric-pressure air (0.1 MPa).
- (3) The observation results obtained using a high-speed camera revealed that the arc root was directly discharged to a copper jig from the discharge probe 24 μ s after application of impulse current under reduced-pressure air (0.02 MPa). The result implies that test conditions, including the specimen size, were inadequate for evaluating the lightning damage behavior of CFRP.
- (4) Arc root behavior on the impulse current attachment surface strongly affects lightning strike damage. Results of numerical simulations demonstrated good agreement with the experimentally obtained results for CF/epoxy when incorporating the experimentally estimated time-dependent arc root size.

References

- [1] Kawakami H, Feraboli P. Lightning strike damage resistance and tolerance of scarf-repaired mesh-protected carbon fiber composites, *Composites Part A* 2011;42:1247–1262.
- [2] Soulas F, Espinosa C, Lachaud F, Guinard S, Lepetit B, Revel I, Duval Y. A method to replace lightning strike tests by ball impacts in the design process of lightweight composite aircraft panels, *International Journal of Impact Engineering* 2018;111:165–176.
- [3] Hirano Y, Katsumata S, Iwahori Y, Todoroki A. Artificial lightning testing on graphite/epoxy composite laminate, *Compos. Part A Appl. Sci. Manuf.* 2010;41:1461–1470.
- [4] Li Y, Li R, Lu L, Huang X. Experimental study of damage characteristics of carbon woven fabric/epoxy laminates subjected to lightning strike, *Composites Part A* 2015;79:164–175.
- [5] Feraboli P, Miller M. Damage resistance and tolerance of carbon/epoxy composite coupons subjected to simulated lightning strike, *Composites Part A* 2009;40:954–967.

- [6] Yamashita S, Sonehara T, Takahashi J, Kawabe K, Murakami T. Effect of thin-ply on damage behavior of continuous and discontinuous carbon fiber reinforced thermoplastics subjected to simulated lightning strike, *Composites Part A* 2017;95:132–140.
- [7] Hirano Y, Yokozeki T, Ishida Y, Goto T, Takahashi T, Qian D. Lightning damage suppression in a carbon fiber-reinforced polymer with a polyaniline-based conductive thermoset matrix, *Compos. Sci. Technol.* 2016;127:1–7.
- [8] Rehbein J, Wierach P, Gries T, Wiedemann M. Improved electrical conductivity of NCF-reinforced CFRP for higher damage resistance to lightning strike, *Composites Part A* 2017;100:352–360.
- [9] Ogasawara T, Hirano Y, Yoshimura A. Coupled thermal–electrical analysis for carbon fiber/epoxy composites exposed to simulated lightning current, *Composites Part A* 2010;41:973–981.
- [10] Abdelal G, Murphy A. Nonlinear numerical modelling of lightning strike effect on composite panels with temperature dependent material properties, *Compos. Struct.* 2014;109:268–278.
- [11] Dong Q, Guo Y, Sun X, Jia Y. Coupled electrical–thermal–pyrolytic analysis of carbon fiber/epoxy composites subjected to lightning strike, *Polym (United Kingdom)* 2015;56:385–394.
- [12] Dong Q, Guo Y, Chen J, Yao X, Yi X, Ping L, Jia Y. Influencing factor analysis based on electrical–thermal–pyrolytic simulation of carbon fiber composites lightning damage, *Compos. Struct.* 2016;140:1–10.
- [13] Wang F.S, Ding N, Liu Z.Q, Ji Y.Y, Yue Z.F. Ablation damage characteristic and residual strength prediction of carbon fiber/epoxy composite suffered from lightning strike, *Compos. Struct.* 2014;117:222–233.
- [14] Wang F.S, Ji Y.Y, Yu X.S, Chen H, Yue Z.F. Ablation damage assessment of aircraft carbon fiber/epoxy composite and its protection structures suffered from lightning strike, *Compos. Struct.* 2016;145:226–241.
- [15] Fu K, Ye L, Chang L, Yang C, Zhang Z. Modelling of lightning strike damage to CFRP composites with an advanced protection system. Part I: Thermal–electrical transition, *Compos. Struct.* 2017;165:83–90.
- [16] Kamiyama S, Hirano Y, Ogasawara T. Delamination analysis of CFRP laminates exposed to lightning strike considering cooling process, *Compos. Struct.* 2018;196:55–62.
- [17] Chemartin L, Lalande P, Peyrou B, Chazottes A, Elias P.Q, Delalondre C, Cheron B.G, Lago F. Direct Effects of Lightning on Aircraft Structure: Analysis of the Thermal, Electrical and Mechanical Constraints, *J. Aerosp. Lab.* (2012) 1–15.
- [18] Kamiyama S, Hirano Y, Okada T, Ogasawara T. Lightning strike damage behavior of carbon fiber reinforced epoxy, bismaleimide, and polyetheretherketone composites, *Compos. Sci. Technol.* 2018;161:107–114.
- [19] SAE Committee report: ARP-5412, Aircraft Lightning Environment and Related Test Waveforms Standard, 1999.
- [20] Latham R.V, *High Voltage Vacuum Insulation: Basic Concepts and Technological Practice*, Academic Press, 1995.

[21] Foster P, Abdelal G, Murphy A. Understanding how arc attachment behaviour influences the prediction of composite specimen thermal loading during an artificial lightning strike test, *Compos. Struct.* 2018;192:671–683.

Acknowledgments

This work was supported by JSPS KAKENHI Grant Numbers 19H02342, 19J22413, and 17K14881. We extend our special thanks to Mr. Hiromitsu Miyaki of JAXA, Mr. Katsunori Takita of IHI Jet Service Co., Ltd., Mr. Tatsuya Shimoe of Tokyo Composite Design & Manufacturing (TCM, Japan) and Mr. Ryuunosuke Minegishi, a graduate student of Tokyo University of Agriculture and Technology, for their technical support.

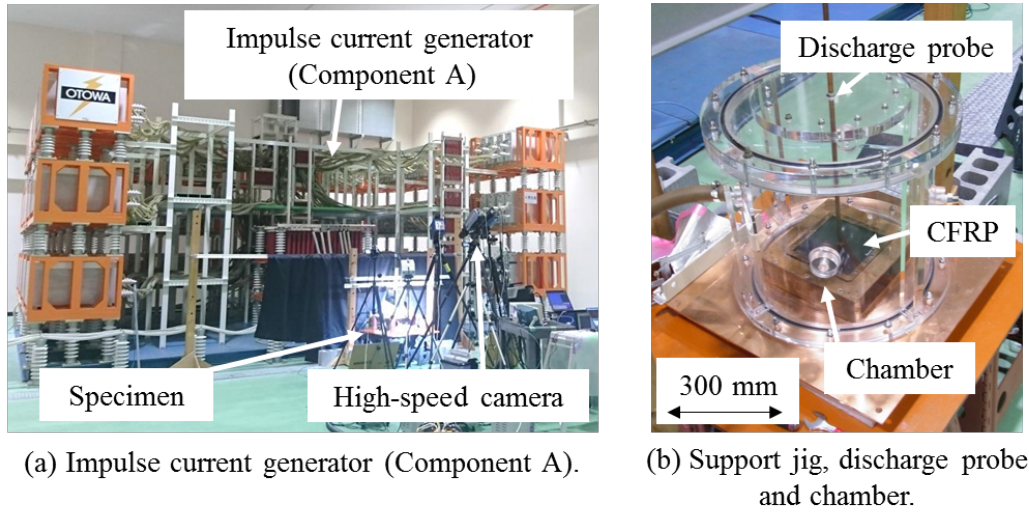


Fig. 1 Experiment setup for simulated lightning current tests.

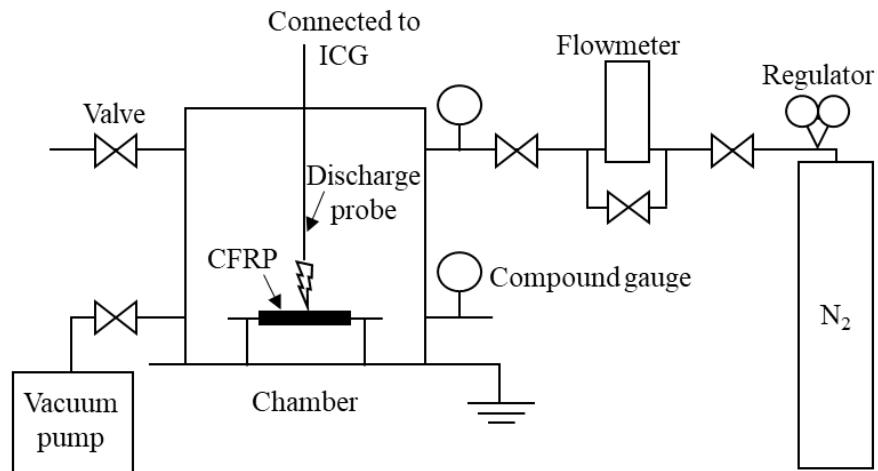


Fig. 2 Schematic drawing of setup for impulse current testing under N₂.

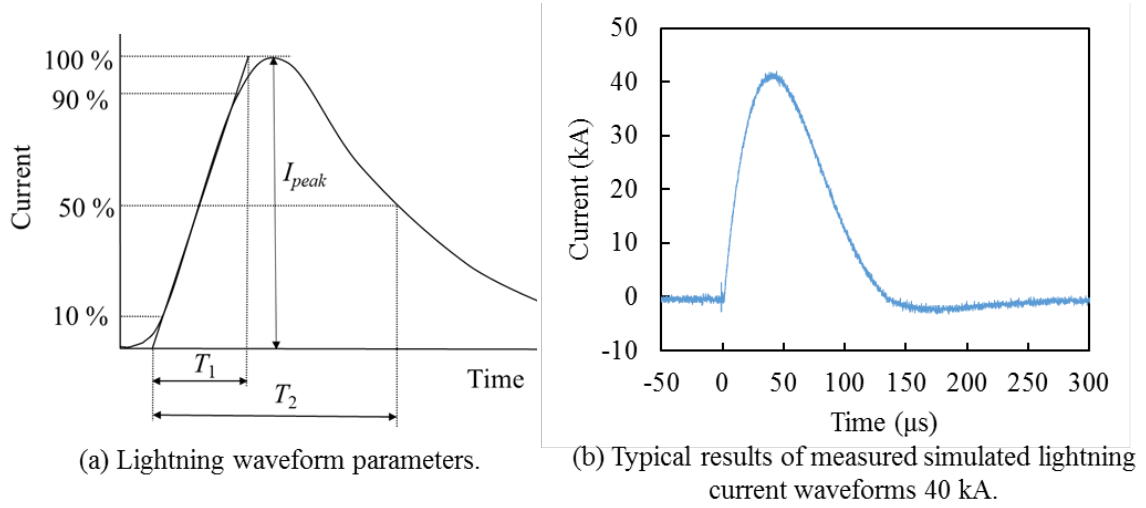


Fig. 3 Lightning waveform.

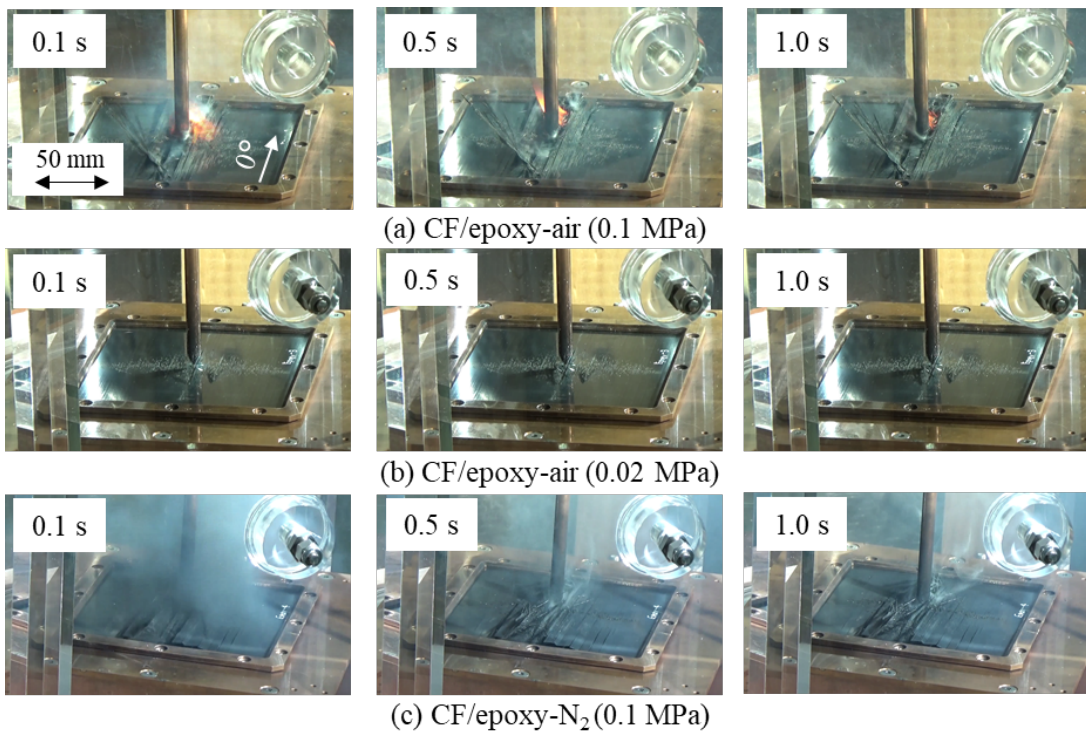


Fig. 4 Experiment results captured by video camera (30 fps) in CF/epoxy.

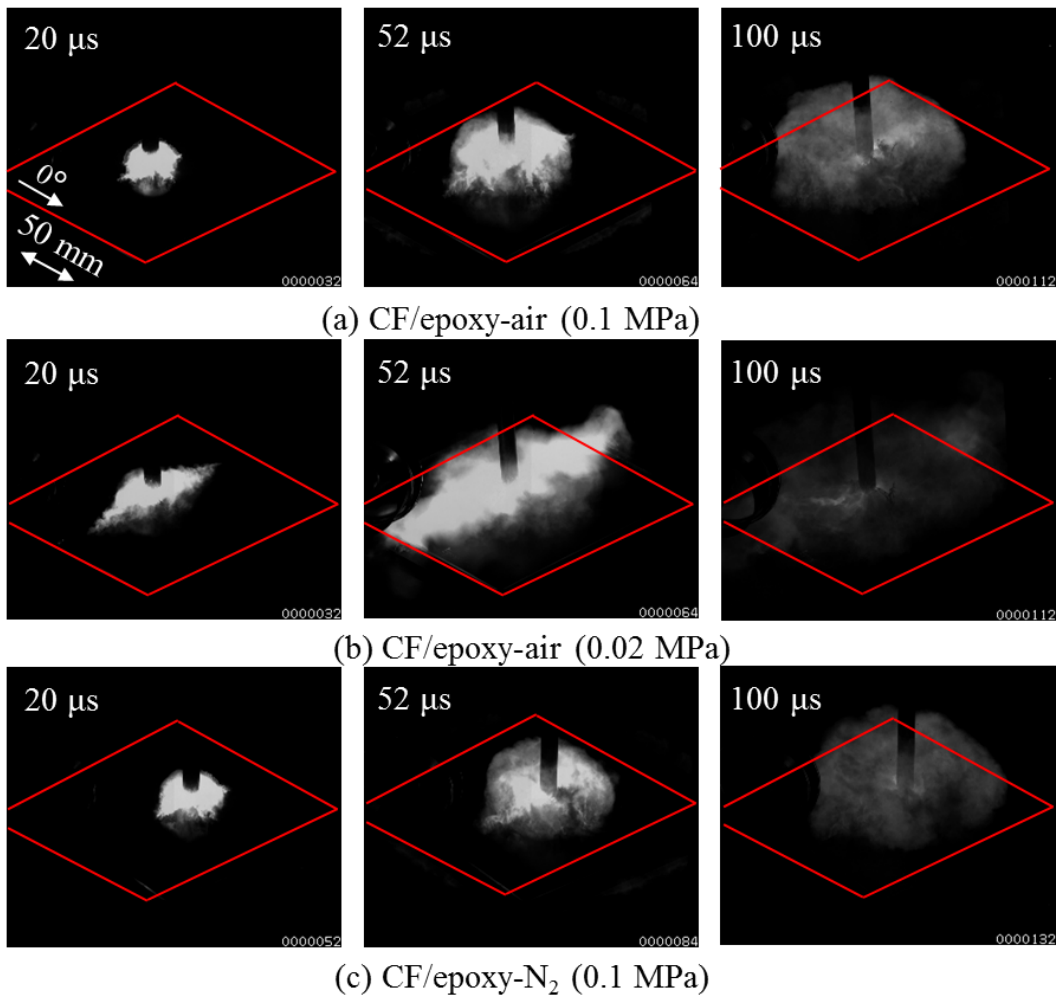


Fig. 5 Experiment results of high-speed camera observation in CF/epoxy. The red line represents the copper jig.

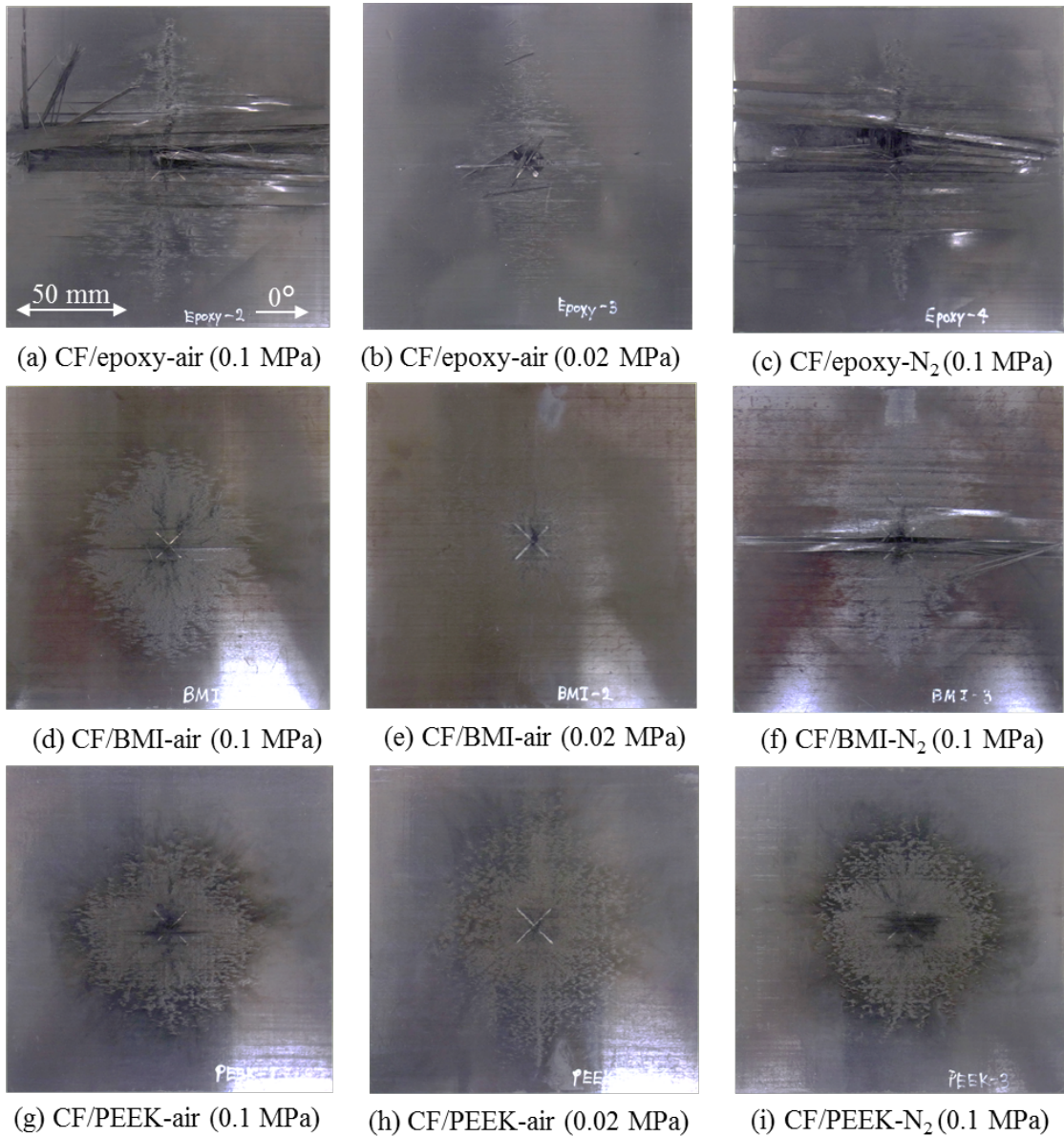


Fig. 6 Arc attachment surface.

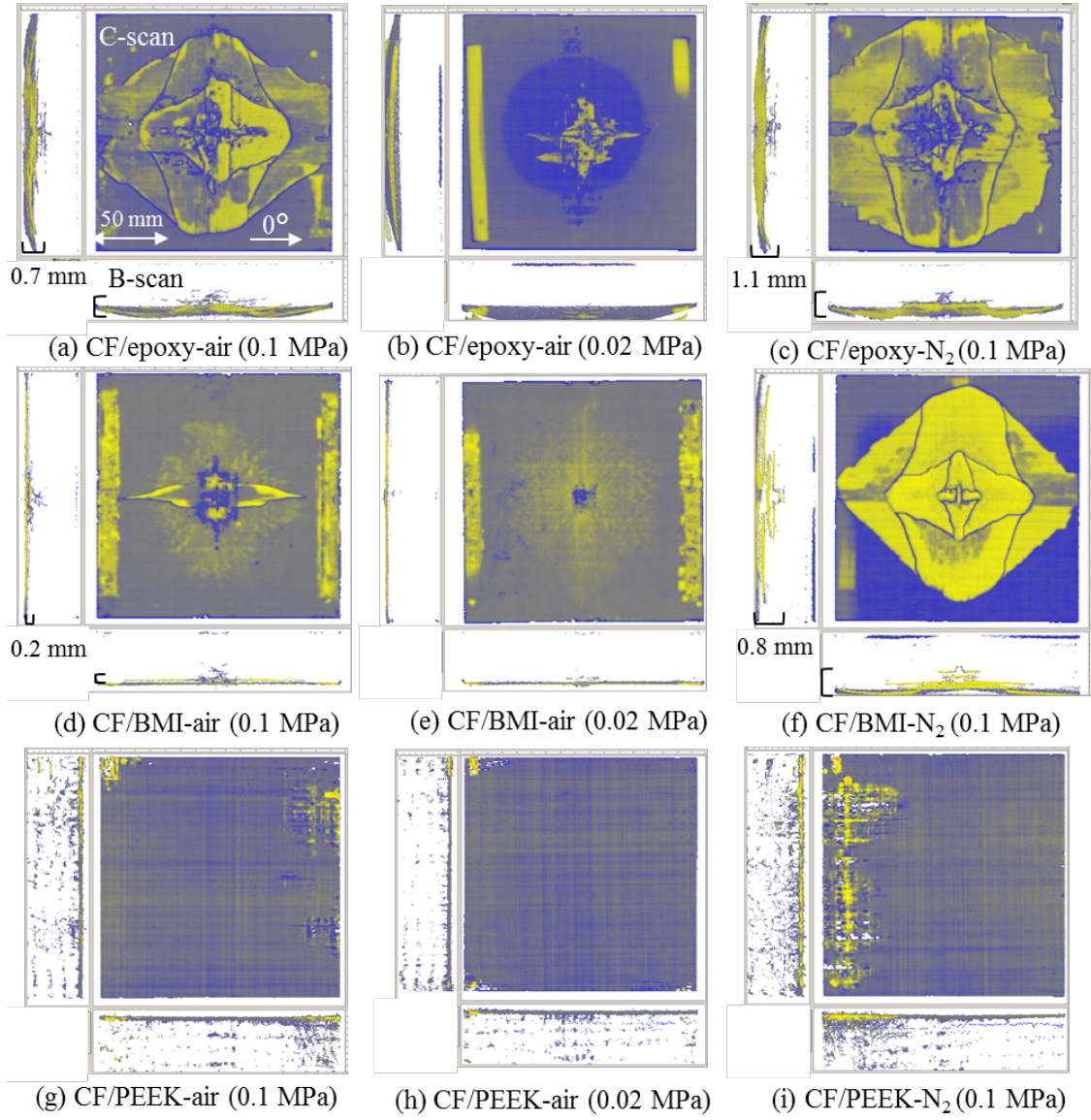


Fig. 7 Ultrasonic inspection results obtained from the back surface.

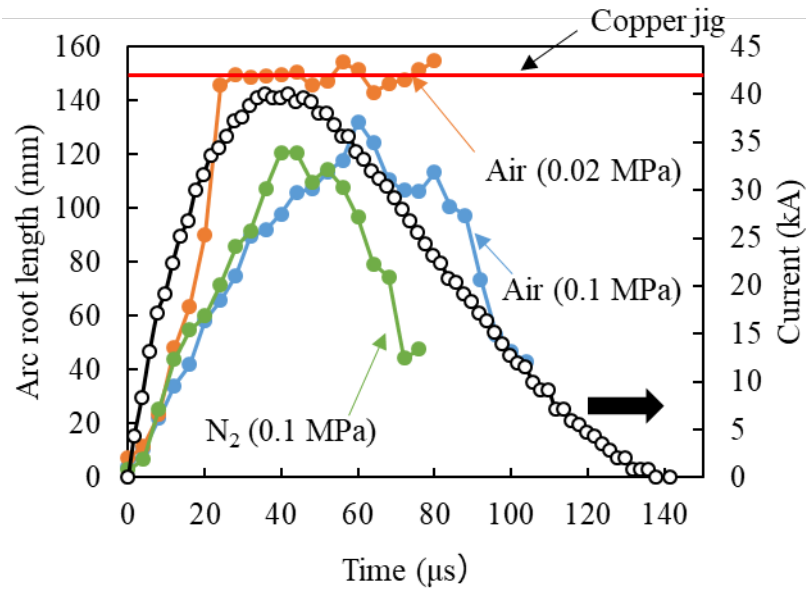


Fig. 8 Arc root length in transverse direction of the top layer in CF/epoxy.

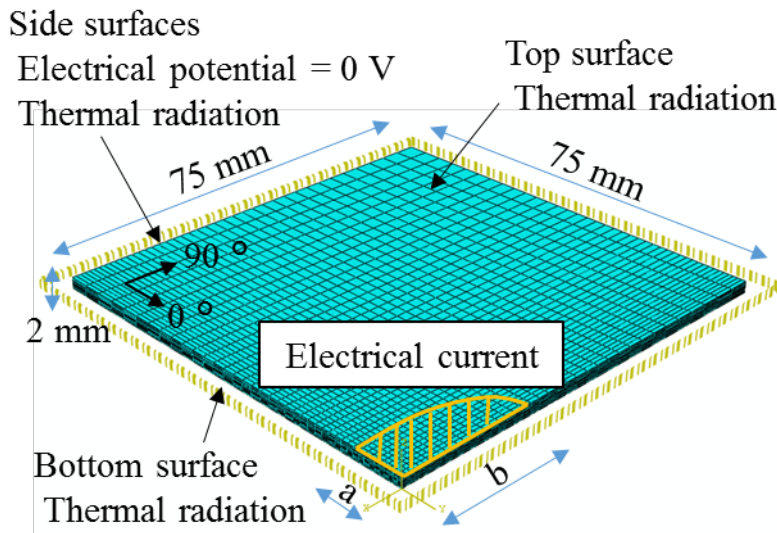


Fig. 9 FEA model and boundary conditions.

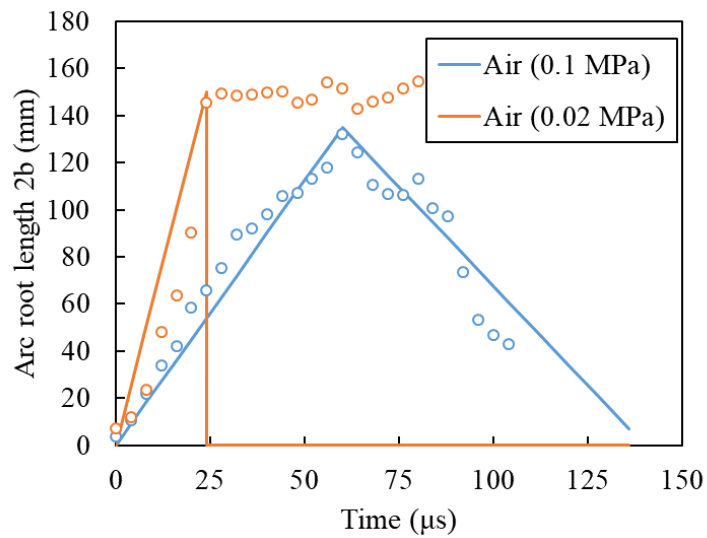


Fig. 10 Arc root length in the transverse direction of the top layer. Symbols show data obtained from experiments using a high-speed camera. Lines show data used for FEA.

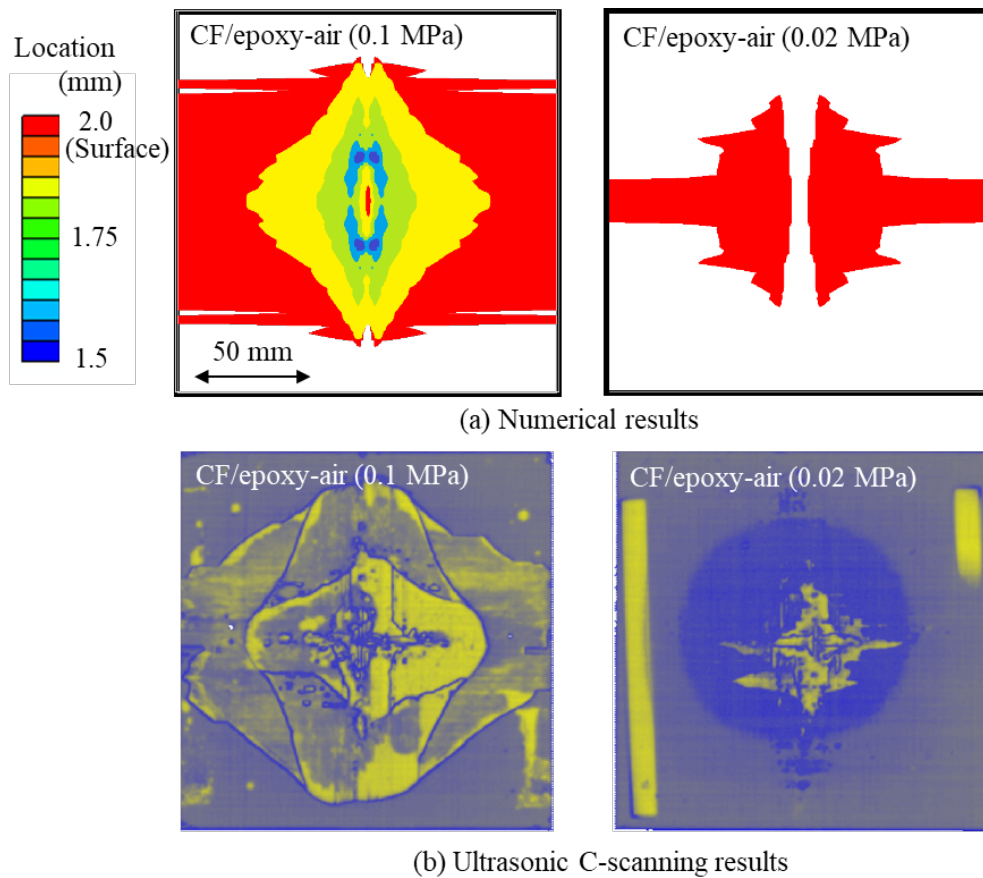


Fig. 11 Superimposed images of contour plots showing the degree of pyrolysis 30 s after impulse current application.

Table 1 Material properties of CF/epoxy, CF/BMI and CF/PEEK

Material	Carbon fiber	Matrix resin	Thickness (mm)	Vf (%)
CF/epoxy	IMS60	#133 (epoxy)	2.2	59
CF/BMI	IMS60	#304 (BMI)	2.1	62
CF/PEEK	IMS60	Victrex PEEK 150G	2.2	59

Table 2 Testing conditions for applied simulated lightning currents

Material	Atmosphere and pressure	Peak current I_{peak} (kA)	Waveform T_1/T_2 (μ s)	Action integral (kA ² s)
CF/epoxy	Air (0.1 MPa)	41.2	27.5/87.4	91.8
	Air (0.02 MPa)	43.0	29.7/88.0	100
	N ₂ (0.1 MPa)	41.0	27.8/86.2	85.9
CF/BMI	Air (0.1 MPa)	42.0	27.7/85.5	93.7
	Air (0.02 MPa)	43.0	28.1/85.1	94.8
	N ₂ (0.1 MPa)	42.0	27.5/85.5	93.0
CF/PEEK	Air (0.1 MPa)	42.0	27.8/85.2	90.3
	Air (0.02 MPa)	42.6	27.8/86.3	95.2
	N ₂ (0.1 MPa)	42.6	28.2/86.1	94.5

Table 3 Internal damage area caused by a simulated lightning strike

Material	Atmosphere and pressure	Damage area (mm ²)
CF/epoxy	Air (0.1 MPa)	13403
	Air (0.02 MPa)	0
	N ₂ (0.1 MPa)	17938
CF/BMI	Air (0.1 MPa)	1340
	Air (0.02 MPa)	0
	N ₂ (0.1 MPa)	12062
CF/PEEK	Air (0.1 MPa)	0
	Air (0.02 MPa)	0
	N ₂ (0.1 MPa)	0